Biophysical Chemistry 245 (2019) 34–40

Contents lists available at ScienceDirect

Biophysical Chemistry

journal homepage: www.elsevier.com/locate/biophyschem

Molecular mechanisms for the destabilization of model membranes by islet amyloid polypeptide

Madhihalli Basavaraju Divakara[a,b,1], Denis Martinez[c,1], Ashwini Ravi[a,b], Veer Bhavana[a,b], Venkata Ramana[d], Birgit Habenstein[c,*], Antoine Loquet[c,*], Mysore Sridhar Santosh[a,*]

[a] Center for Incubation, Innovation, Research and Consultancy (CIIRC), Jyothy Institute of Technology, Thataguni, Off Kanakapura Road, Bangalore 560082, Karnataka, India
[b] Visvesvaraya Technological University, Regional Research Centre, Jnana Sangama, Belagavi 590018, Karnataka, India
[c] Institute of Chemistry and Biology of Membranes and Nanoobjects, Institut Européen de Chimie et Biologie (CNRS UMR 5248), Université de Bordeaux, 2 Rue Robert Escarpit, 33600 Pessac, France
[d] DRDO BU CLS, Bharathiar University Campus, Coimbatore 641046, Tamil Nadu, India

HIGHLIGHTS

- Human islet amyloid polypeptide (hIAPP) is a peptide known to aggregate into oligomers and amyloid fibrils.
- Real-time microscopy shows a time-dependent penetration of hIAPP oligomers into liposomes.
- Deuterium NMR reveals a lipid ordering in presence of hIAPP.
- Oligomeric species, rather than fibrils, are responsible for membrane destabilization.

GRAPHICAL ABSTRACT

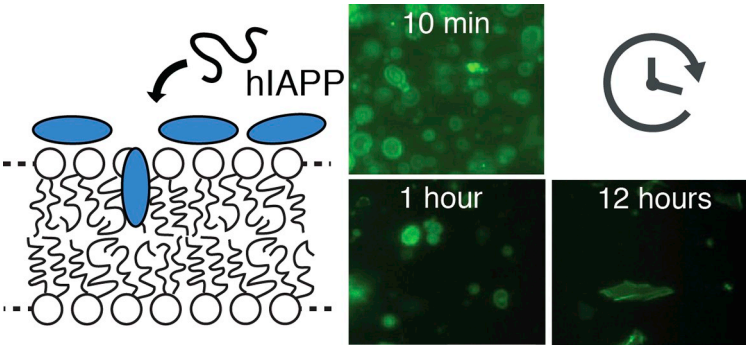

ARTICLE INFO

Keywords:
Type 2 diabetes
IAPP
ssNMR
Oligomers
Fibrillation
Membrane destabilization
Islet amyloid polypeptide
NMR spectroscopy
Lipid-protein interaction
Amyloid fibrils

ABSTRACT

Misfolding of human islet amyloid polypeptide (hIAPP) into insoluble aggregates is associated with Type 2 diabetes. It has been suggested that hIAPP toxicity may be due to its accumulation in pancreatic islets, causing membrane disruption and cell permeabilization, however the molecular basis underlying its lipid association are still unclear. Here, we combine solid-state NMR, fluorescence and bright field microscopy to investigate hIAPP - lipid membrane interactions. Real-time microscopy highlights a time-dependent penetration of hIAPP oligomers toward the most buried layers of the lipid vesicles until the membrane disrupts. Deuterium NMR was conducted on liposomes at different hIAPP concentration to probe lipid internal order and thermotropism. The gel-to-fluid phase transition of the lipids is decreased by the presence of hIAPP, and site-specific analysis of the order parameter showed a significant increase of lipid order for the first eight positions of the acyl chain, suggesting a partial insertion of the peptide inside the bilayer. These results offer experimental insight into the membrane destabilization of hIAPP on model membrane vesicles.

* Corresponding authors.
E-mail addresses: b.habenstein@iecb.u-bordeaux.fr (B. Habenstein), antoine.loquet@u-bordeaux.fr, a.loquet@iecb.u-bordeaux.fr (A. Loquet), santoshgulwadi@gmail.com (M.S. Santosh).
[1] MBD and DM contributed equally to this work.

https://doi.org/10.1016/j.bpc.2018.12.002
Received 5 September 2018; Received in revised form 29 November 2018; Accepted 10 December 2018
Available online 14 December 2018

1. Introduction

Amyloids are proteinaceous deposits observed as unbranched filaments at the macroscopic level, often bearing a typical cross-beta signature as seen by X-ray diffraction analysis [1]. Many amyloid proteins and peptides are associated with the propagation of neurodenegerative disorders [2,3], through the formation of insoluble amyloid fibrils that are resistant to denaturing conditions. Prior to the growth of mature fibrils, the putative formation of intermediary oligomeric species has been evoked to be the pathogenic agents associated with amyloid-related diseases [4,5], such as in Parkinson's [6], Alzheimer's [7,8,9] and Type 2 diabetes [10,11,12] pathologies. Oligomers of amyloid proteins constitute very challenging targets for biophysical techniques due to their inherent heterogeneous nature [13], leading to important local structural polymorphism.

Among the ~40 amyloid proteins involved in human disorders [14], the islet amyloid polypeptide (IAPP or amylin) is associated with type 2 diabetes [15,16]. The human IAPP (hIAPP) is a 37-residue peptide neuroendocrine hormone co-secreted and co-localized with insulin in pancreatic islet β-cells. Its aggregation in pancreatic islets and disruption of β-cells is the hallmark of type 2 diabetes [17–19], characterized by a chronic insulin resistance and a progressive loss of β-cells [20,21]. The misfolding of hIAPP leads to the formation of extracellular plaques and extended amyloid fibrils that have been linked to β-cell death in Type 2 diabetes [22,23]. The deposited amyloid fibrils are composed of β-sheet aggregates with the characteristic structural features [24–26] similar to those found in Alzheimer's, Parkinson's, Prion diseases and a variety of other neurodegenerative disorders. It has been suggested that IAPP mediates cellular membrane damage leading to the permeabilization and disruption of membranes in pancreatic β-cells. Previous results suggested that hIAPP toxicity is primarily related to its destabilizing effects on lipid membranes [27–32]. Although the molecular mechanisms of hIAPP toxicity are still under debate, the fact that oligomeric species can be formed early during the aggregation process and might interfere with the lipid bilayer stability has been proposed by Ramamoorthy and coworkers [33]. Several hypothesis related to the formation of membrane pores [28,34], in analogy to ion-channels, or to direct membrane disruption [35–37], have been proposed to explain hIAPP-dependent membrane damage. It is known that the interactions between amyloid-forming peptides and their fragments with lipids are responsible for membrane destabilization. The pre-fibrillar complexes involved in these interactions appear early in the fibrillation pathway and are found to be the cytotoxic species during amyloid formation [28]. The mature amyloid fibrils are thought to replace β-cell mass and are less cytotoxic than the soluble oligomers [35,38]. The initial process of membrane disruption by hIAPP still remains an unchartered field.

In this study, biophysical investigations of membrane destabilization induced by hIAPP aggregates have been engaged. Various biophysical techniques including solid-state NMR (ssNMR) spectroscopy, ThT assay, fluorescence and confocal microscopy were used to monitor hIAPP – membrane interactions at various scales. ssNMR spectroscopy provides insights into the effect of different hIAPP doses on membrane fluidity and lipid thermotropism, whereas fluorescence microscopy allows for visualization of the morphology of liposomes and their surface changes upon addition of the peptide. We here attempt understanding the perturbation of lipid membrane in the presence of hIAPP and reconstituting the determining factors of amyloid disease progression *in vitro*.

2. Materials and methods

2.1. Chemical reagents

1, 2-dimyristoyl-d_{54}-*sn*-glycero-3-phosphocholine (DMPC-d_{54}) and 1, 2-dimyristoyl-*sn*-glycero-3-phosphocholine (DMPC) were purchased from Avanti Polar Lipids, Inc. (USA) stored at a temperature of −20 °C. Dimethyl sulfoxide (DMSO) and Thioflavin-T (ThT) were purchased from Sigma-Aldrich and hIAPP with 95% purity (HPLC data provided as supplementary material) was purchased from GL Biochem (Shanghai) Ltd., China.

2.2. Liposome sample preparation

Multi-lamellar vesicles (liposomes) were prepared by dissolving 10 mg of pure DMPC-d_{54} in chloroform to get a clear solution. Chloroform was then evaporated under vacuum. Solvent free lipid was hydrated with ultra-pure water and subjected to lyophilisation overnight. Further, lipid powder was rehydrated with 40 μL of deuterium-depleted water and subjected to 3 cycles of vigorous shaking in a vortex mixer (3000 rpm), freezing (−196 °C, liquid nitrogen,1 min) and thawing (40 °C, in a water bath, 10 min) for homogenization. Liposomes containing hIAPP were prepared in the same way by mixing DMPC-d_{54} and hIAPP powders in chloroform (hIAPP:lipid proportion of 1:10, 1:30 and 1:100) followed by evaporation of chloroform under vacuum and overnight lyophilization. For liposomes containing 30% cholesterol (molar ratio), lipid powders were solubilized in chloroform/methanol mixture (2,1) and we followed the same procedure previously described. The lyophilized samples were hydrated to a hydration ratio of 80% according to the composition.

2.3. Solid state NMR spectroscopy

The samples were filled into 4 mm ssNMR rotors before data acquisition. ^{2}H NMR studies were carried out on Bruker Avance II 500 MHz WB (11.75 T) and Avance II 400 MHz (9.4 T) spectrometers. ^{2}H NMR experiments on ^{2}H-labeled DMPC were performed with a phase-cycled quadrupolar echo pulse sequence (90°x-τ-90°y-τ-acq). ^{31}P NMR spectra were recorded using a phase-cycled Hahn-echo pulse sequence (90°x-τ-180°x/y-τ-acq). Acquisition parameters were as follows: 250 kHz spectral width for ^{2}H NMR and 64 kHz for ^{31}P NMR spectroscopy, π/2 pulse width of 2.62 for ^{2}H and 8 μs for ^{31}P, interpulse delays τ were of 40 μs, recycled delays were 1.3 s for ^{2}H and 2 s for ^{31}P, 800 to 2048 scans were recorded depending on the samples. A Lorentzian line broadening of 200 Hz for deuterium spectra was applied before Fourier transformation from the top of the echo. Samples were allowed to equilibrate at least 30 min at a given temperature prior to data acquisition. All the spectra were processed and analysed using Topspin 3.2 software (Bruker Biospin). Spectra moments were determined for each temperature by using NMR Depaker 1.0rc1 software (Copyright © 2009 Sebastien Buchoux). Orientational order parameters (S_{CD}) were calculated from experimental quadrupolar splittings ($\Delta\nu_Q$) according to the following mathematical relation [Eq. (1)]:

$$\Delta\upsilon_\alpha(0) = \frac{3}{2}\Lambda_\alpha\left(\frac{3\cos^2 0 - 1}{2}\right)Sc_\alpha \quad (1)$$

with $A_Q = (e^2qQ)/h$, the quadrupolar coupling constant for methyl moeities (167 kHz) and the angle between the magnetic field and the bilayer normal [14]. The order parameter was calculated as a mean for the structural order along the bilayer normal.

2.4. Fluorescence microscopy

Fluorescence microscopy and ThT assay studies were performed on liposomes of pure DMPC prepared by hydration of 10 mg of chloroform evaporated lipid with 100 μL of ultrapure water and submitted to 5 cycles of vigorous shaking in a vortex mixer (3000 rpm). The sample was frozen to −196 °C and immediately subjected to overnight lyophilisation. It was rehydrated to 80% hydration ratio and subjected to 3 cycles of freezing (−196 °C for 2 min) and thawing (40 °C for 10 min) for homogenization. It was then diluted to 10 times of the hydrated volume with ultra-pure water prior to fluorescence imaging. Both ThT

and hIAPP was dissolved in 0.8% (DMSO *v*/v) and the final concentration was made up to 200 μM with PBS (pH 7.4) was initially added to the prepared liposomes and were then transferred in 96-well plates, incubated at room temperature for 10 min and were observed under an INCell Analyzer 6000 (GE Healthcare), 60× 0.70 NA air objectives, fitted with an sCMOS 5.5 Mp camera, with an x − y pixel separation of 108 nm. The acquired images were colorized without adjusting the contrast by using Fiji ImageJ software and were processed under similar conditions. The same method as above was used to prepare the sample but without adding ThT to avoid fluorescent dye interaction during light microscopic (bright field) imaging.

2.5. Thioflavin T preparation, fluorescence measurement and fluorescence microscopy

Multi-lamellar vesicles were prepared by co-solubilizing DMPC and hIAPP as described in the NMR experiments and were diluted 10 times before subjecting it to ThT assay where the molar ratio of hIAPP:DMPC was 1:30. ThT fluorescence was measured using a SYNERGY microplate reader and the measurement parameters used were as follows: excitation - 440 nm and emission - 485 nm at ambient temperature. ThT fluorescence on hIAPP was performed at a hIAPP: ThT ratio of 1:1. A control experiment was made to determine the ThT contribution by measuring the fluorescence in absence of ThT.

3. Results

3.1. Solid-state NMR spectroscopy probes lipid ordering, thermotropism and membrane destabilization in presence of hIAPP

Membrane vesicles were reconstituted incorporating deuterated phosphatidylcholine lipids (DMPC-d_{54}) and cholesterol using standard freeze-thaw cycles to produce homogeneous liposomes. Prior to liposome formation, hIAPP peptides were incorporated by co-solubilization with the lipids. The hydrated liposomes were then subjected to ssNMR spectroscopy to trace the potential effect of hIAPP on lipid internal ordering, thermotropism and polymorphism. ^{31}P-detected ssNMR spectroscopy is a powerful tool to characterize membrane polymorphism as phospholipid headgroups naturally contain phosphorus. By measuring the width of ^{31}P NMR spectra, the lipid headgroup mobility and orientation can be assessed, given by the chemical shift anisotropy (CSA). To monitor the influence of hIAPP on liposomes surface, ^{31}P ssNMR spectra of DMPC liposomes were acquired with or without hIAPP at different peptide/lipid ratio (Fig. 1). All spectra exhibit a comparatively similar powder line shape: a broad anisotropic ^{31}P ssNMR signal with a pronounced peak at high field and a less intense shoulder at the low field edge. This shape and width are typical for phospholipids organized in a lamellar phase [39]. Therefore, we can infer from these results that the lipid remains in its lamellar phase in spite of the presence of hIAPP. The interaction of hIAPP with the membranes slightly changes the CSA values of DMPC at 298 K and 310 K (from 41.1 to 43.0 ppm at 298 K and from 44.6 to 40.2 ppm at 310 K, with a precision of ± 0.5 ppm), while the same CSA values were observed even at a high peptide/lipid molar ratio. The CSA change could be interpreted as a modification of the local electronic environment, of the lipid head group or in the head group mobility. In this case, even the here-tested unrealistic high peptide concentration (1:10) results in minimal interactions with the lipid headgroups.

To investigate the effect of hIAPP on lipid internal dynamics and global membrane thermotropism, static ^{2}H NMR was performed on vesicles incorporating deuterated DMPC lipids. Fig. 2A shows selected ^{2}H spectra acquired at 298 K, above the phase transition temperature of DMPC-d_{54} (20 ± 1 °C). Narrow ^{2}H line-widths and well resolved individual Pake doublets were observed, indicating typical lamellar phase. For the highest peptide/lipid ratio (1/10), a large line broadening is observed, corresponding to a decrease of the C-D bonds

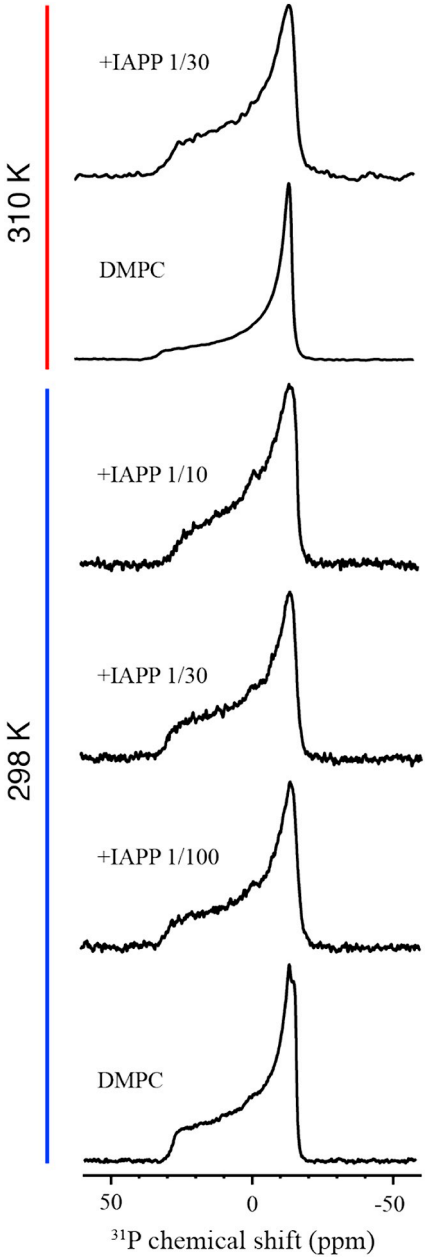

Fig. 1. ^{31}P solid-state NMR experiments of pure DMPC liposomes and hIAPP co-solubilized with DMPC liposomes at different peptide/lipid ratio (1/100; 1/30; 1/10). The spectra corresponding to as peptide/lipid ratio of 1:30 were acquired at 298 K and 310 K. A Lorentzian line broadening of 50 Hz was applied before the Fourier transformation.

motions. A detailed analysis of the lipid internal motions was carried out by measuring the structural order parameter (S_{CD}) along the acyl chain, as a function of the carbon position. The S_{CD} is calculated for each carbon position using experimental quadrupolar splittings (Dn_Q). Fig. 2C shows the $|2S_{CD}|$ values as a function of the labeled carbon positions. The results reveal a typical behavior for lamellar phases with a high structural order for the very restrained glycerol backbone (2 to 8) followed by a decrease of the order toward the center of the membrane. Addition of hIAPP (red lines) increases the lipid order compared to pure DMPC-d_{54} liposomes (blue line). While at 1/30 and 1/10 ratios, the peptide only affects the first 8 positions (dotted lines), the ordering effect is more important at a 1/100 ratio. Firstly, the absolute $|2S_{CD}|$ values are higher, and secondly, positions 2 to 12 are significantly affected. We therefore hypothesized that the penetration of the peptide in

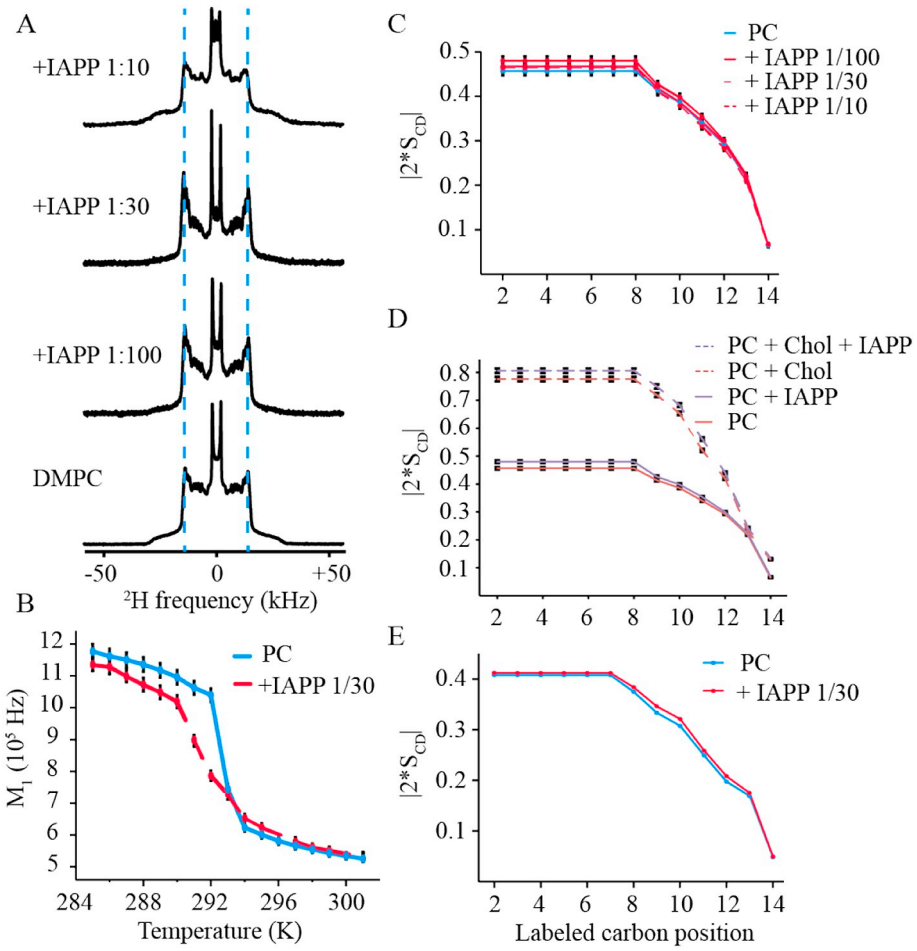

Fig. 2. Lipid ordering of hIAPP probed by ^{2}H solid-state NMR experiments, performed at a peptide/lipid ratio of 0:100, 1:100, 1:30, and 1:10, (A) Wide-line ^{2}H spectra of PC liposomes containing hIAPP. (B) Variation of the first spectral moment as a function of the sample temperature. C—^{2}H order parameters of the PC acyl chain as a function of the carbon position. De-Pake-ing and simulations were applied on ^{2}H solid-state NMR spectra acquired at 298 K to determine accurately individual quadrupolar splittings. |SCD| order parameters of DMPC-d54 acyl chain were derived from experimental quadrupolar splittings and plotted as a function of labeled carbon position for DMPC liposomes (blue) and DMPC with IAPP (red) at different peptide/lipid ratio (1:100, solid line; 1:30, longdash; 1:10, dotted). (D) Comparison of the C—^{2}H order parameters of the PC acyl chain with (dashed lines) or without 30% cholesterol (solid lines) in the presence (blue) or not (red) of IAPP (1:30 peptide/lipid molar ratio). (E) Effect of IAPP on the DMPC C—^{2}H order parameter at 310 K. (For interpretation of the references to colour in this figure legend, the reader is referred to the web version of this article.)

the membrane might be much more efficient at low concentration. However, at higher concentrations, the ordering effect becomes less pronounced, probably because the peptide tends to interact both with itself and the membrane. We carried out the same experiments at a 1/30 IAPP/Lipid molar ratio with liposomes containing 30% cholesterol (Fig. 2D) to mimic the membrane rigidity of eukaryotic cells. We observed a significant increase of the local order parameter along the acyl chain in the presence of hIAPP, affecting the first 12 positions. This effect is slightly higher compared to cholesterol-free membranes, suggesting that hIAPP is still able to intercalate between lipid acyl chains, despite the presence of cholesterol and the high rigidity of the membrane. We note that the rigidifying effect of hIAPP on the PC membranes is however a factor less compared to the well-known effect of cholesterol on membrane ordering.

The spectral moment (M_1) was measured at different temperatures to describe the thermotropic behaviour of DMPC-d_{54}, in the presence of hIAPP at 1/30 ratio (Fig. 2B). As this parameter is related to the average value of the S_{CD}, it gives an insight into the global lipid dynamics of the membrane bilayer. The higher is the structural order, the higher is the M_1. Fig. 2B shows the variation of M_1 as a function of the temperature. The blue line indicates the thermotropic behaviour of pure DMPC liposomes. Below the phase transition temperature (under 293 K *i.e.* in the gel phase), lipid chains are tightly packed and display high M_1 values. The values decrease as a function of the temperature and a sudden transition is observed between 292 and 294 K. The gel-to-fluid phase transition temperature is determined at the inflection point of the curve, here 293 K. The same experiments were conducted in the presence of hIAPP at a 1/30 ratio. If the gel phase of the lipid bilayer is already disordered due to the interfering effects of hIAPP, then the heat required for the transition is lowered (between 290 and 294 K) relative to the pure lipid vesicles, which is reflected by the substantial broadening of the phase transition. This suggests that IAPP peptides penetrate until the 8th position of the lipid acyl chain, affects lipid-lipid interactions and decreases the cooperativity of the lipid phase transition. To probe the effect of hIAPP on membrane rigidity in physiological conditions, the same experiments were performed at 310 K (Fig. 2E). However, we did not observe significant differences on the lipid ordering and peptide localization compared to 298 K.

3.2. ThT assay

ThT, a specific dye for amyloidosis, was used to reveal the state of hIAPP aggregation and specific hIAPP fibrillation in the presence of lipids. ThT assay (Fig. 3) showed no differences from previous studies on the progressive development of amyloid and mature fibrils [25,40]. Indeed, hIAPP in PBS buffer showed no detectable fluorescence during the first hours of the experiment. When incubated with PC liposomes, we observed a rapid and linear increase of the fluorescence intensity during the first 200 min. This increase in fluorescence corresponds to the fast conversion of hIAPP soluble monomers to small aggregates. It indicates that the rapid aggregation of hIAPP is induced by peptide-membrane interactions. After 300 min, the fluorescence reaches a plateau for which the oligomeric species of hIAPP are stable before the transition to a mature amyloid fibril. In parallel with the fluorescence spectroscopy assays, we followed potential structural changes of the lipid vesicles at different incubation times using light microscopy.

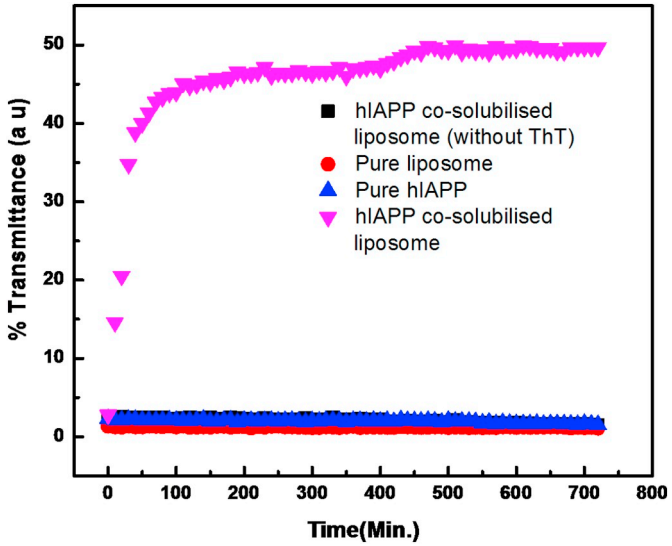

Fig. 3. hIAPP fibrillation process was monitored by ThT fluorescence assay incubating sample at 298 K performed on: DMPC liposome (black), hIAPP (red), liposome and hIAPP without ThT (blue), liposome and hIAPP (magenta). (For interpretation of the references to colour in this figure legend, the reader is referred to the web version of this article.)

3.3. Fluorescence microscopy

The primary focus here was to study the simultaneous evolution of hIAPP oligomeric state and liposomes morphology upon treatment with hIAPP at 1:30 peptide/lipid ratio. Solid-state NMR studies have previously shown that the concentration of the peptide has minimal effect on the organization of the lipid headgroup at the membrane surface and on the hydrophobic acyl chain, although the membrane order was higher in presence of hIAPP. Real-time bright field images of hIAPP treated vesicles were captured, in which no bright spots were observed immediately (0th min) after the addition of hIAPP (Fig. 4A). Bright white spherical spots of hIAPP were seen on the circumference of liposomes within 10 min after the addition of hIAPP as shown in Fig. 4B. Upon continued incubation for 45 min, the intensity as well as the number of white spots decrease on the surface and translocate toward the inner layers of the vesicles, where curvy aggregates were also detectable (Fig. 4C). Moreover, the changes in sample morphology at two different time intervals of 45 and 150 min are also evident in Fig 4C and D. Curvy and short aggregates of hIAPP are clearly visible at the end of the growing phase. hIAPP localized in the hydrophobic core of the bilayer display a continuous growing over time and form curvy structures, which is a typical behaviour for protofibrils [41], whereas in the absence of hIAPP no such bright spots were seen in the liposomes under similar conditions (Fig. 4E-H). From the Fig. 4D, vesicle-like shape of hIAPP aggregates incorporated into liposomes were still detectable even at the end of the growing phase (150 min). Meanwhile, the morphology of vesicles seemed also to be affected at the beginning of fibrillation itself.

In order to estimate the modification of liposomes morphology during incubation with hIAPP, we conducted fluorescence microscopy of ThT (emits green fluorescent light) stained samples. Fig. 5 shows ThT fluorescence associated to hIAPP oligomers in the context of a membrane environment. During the early stages of the hIAPP aggregation process (10 min), a complete surrounding of the liposomes by hIAPP amorphous aggregates is observed (Fig. 5A) which is evidenced by the presence of green fluorescent background. A longer incubation (1 h, Fig. 5B) revealed a diffusion of the fluorescence from the surface to deeper layers inside the liposomes, confirming the penetration of the hIAPP aggregates. Liposomes can only retain their morphology for few hours after peptide addition, leading to complete membrane disruption once the growing phase ends (Fig. 5C). This co-localization of lipids and peptides in aggregates indicate the final fate of oligomers where they eventually disassociate from the bilayer causing membrane disruption. Mature fibrils with filament-like morphology were observed at 12 h (Fig. 5D). During the process of fibrillation, small hIAPP oligomers in spherical shape were first observed around the membrane surface. These spherical species are believed to be converted into more elongated protofibrils which gradually interact with lipids of the membrane vesicles. The final state observed by fluorescence microscopy reveals that hIAPP fibril-like aggregates adopt a more straight and long fibrillar morphology, typically observed for amyloid fibrils. This difference suggests that fibril formation kinetics would be affected by the

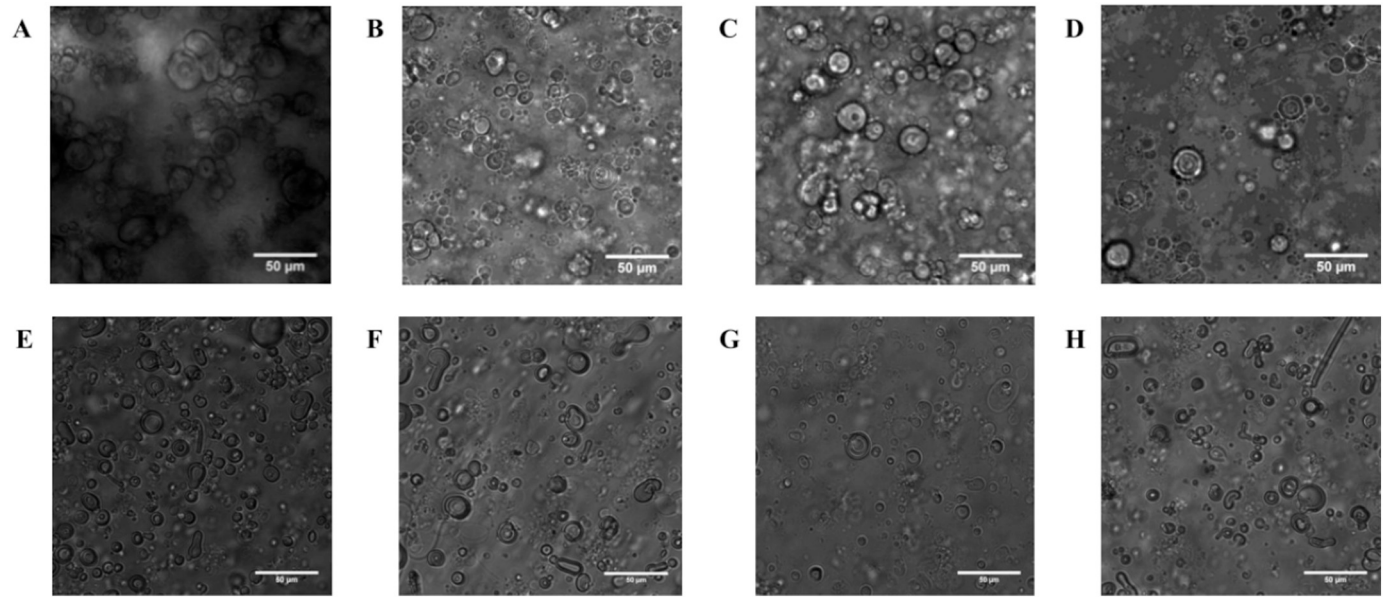

Fig. 4. Real time morphology change in liposomes (1) after addition of hIAPP (A) DMPC liposomes at 0 min (B) 10 min (C) 45 min (D) 150 min; (2) In absence of hIAPP (E) DMPC liposomes at 0 min (F) 10 min (G) 45 min (H) 150 min at room temperature.

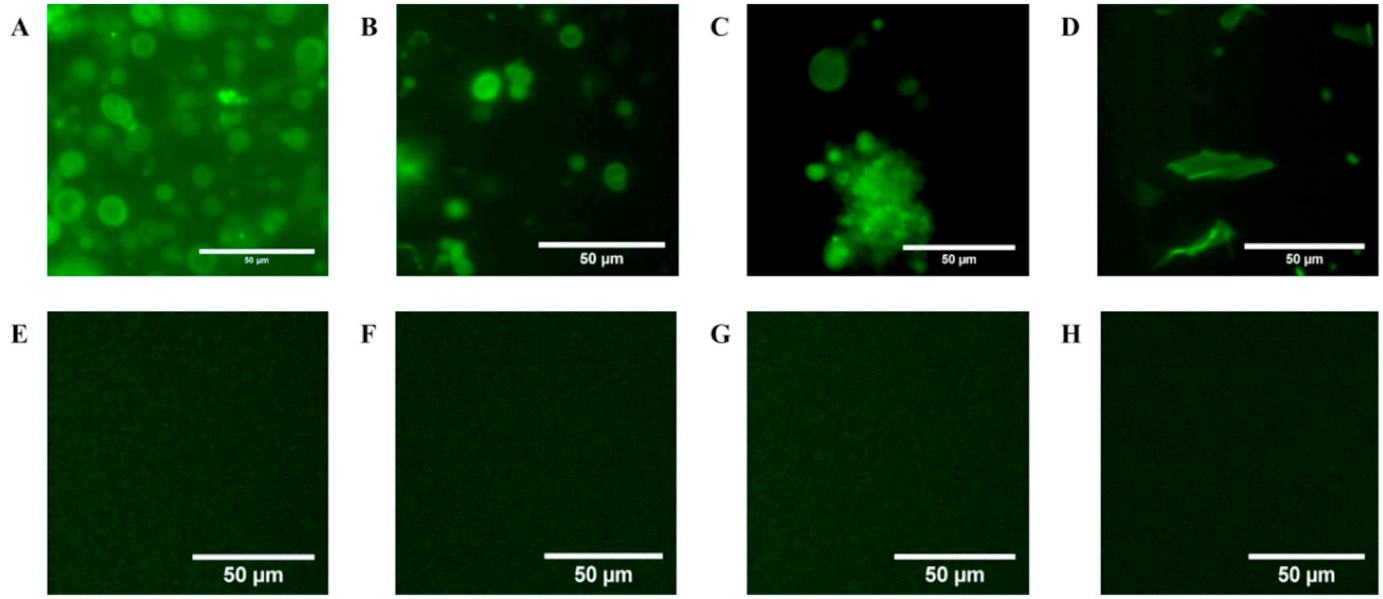

Fig. 5. Real time morphology change in liposomes followed by fluorescence microscopy of ThT stained samples (1) after addition of hIAPP (A) 10 min (B) 1 h (C) 6 h (D) 12 h; (2) In absence of hIAPP (E) 10 min (F) 1 h (G) 6 h (H) 12 h of incubation at room temperature.

membrane composition, presumably related to change in local concentration of hIAPP. ThT fluorescence intensified immediately after the addition of peptides to vesicle solutions. The final morphologies of vesicles upon addition of peptide were long and straight, typically in length of several microns (Fig. 5D). Morphology remained curvy when fibrils extended to several hundreds of nanometers within 150 min. Whereas in the absence of hIAPP, the liposome shows no fluorescence that we can clearly see from Fig. 5(E–H) even after 12 h of incubation. The morphological feature of pre-incorporated fibrils was very similar to a previously observed metastable intermediate formed by the Iowa mutant of amyloid precursor protein [42]. It is possible that the curvy filaments observed in the present work also represent an intermediate morphology before the formation of mature fibrils. In addition, we also observed a difference in terms of the membrane morphology. During the fibrillation process, predominant spherical vesicles and co-ordinative insertion of hIAPP to the hydrophobic core of vesicles were observed at the growing phase, whereas during fibrillation, subsequent loss of lipid from the vesicles resulted in mature fibrils with loss of integrity of the vesicles.

4. Discussion

In this work, we investigate the early molecular events of hIAPP interaction with membrane liposomes. Using a combination of solid-state NMR spectroscopy and time-resolved fluorescence microscopy, we probe the hIAPP-dependent effect on the lipid membrane organization at different scales, using DMPC lipids as a model system to mimic the membrane. The present study provides experimental insights into the appearance of hIAPP species that directly interact with the lipid bilayer of the liposomes. These hIAPP aggregates appear to be transient soluble membrane-active intermediates, interacting with lipids prior to the fibril formation. However, based on our observations by ssNMR and fluorescence microscopy, it can not be ruled out that fibrils also have an effect on the membrane organization. Solid-state NMR data show a very low impact on the lipid organization as seen by minimum order parameter perturbation measured on the acyl chains. However the membrane thermotropism in contact with hIAPP is clearly modified, suggesting that the peptide is associated primarily to the membrane surface. It has been demonstrated that hIAPP peptide can modulate its conformational structure in presence of lipids [43–46] and that its membrane insertion is preferentially taking place in a monomeric state [47]. We observed a small increase of the C—^{2}H order parameters in presence of hIAPP, indicating that the peptide penetration creates a minimum void in the liposomes. However, the thermal variations of the spectral moment are importantly modified in presence of hIAPP, indicating a change in the global membrane fluidity. Consistent with previous observations suggesting that lipids would facilitate the conversion of hIAPP monomers into β-sheet-rich high-order oligomeric species interacting with the membrane [47–49], the hIAPP-lipid interaction observed in this study induce noticeable change in the membrane dynamic organization. The lipid ordering by hIAPP results in the crowding of the hydrophobic region of the bilayer and is probably driven by hydrophobic insertion, as already observed for antimicrobial peptides [50]. As seen by time-resolved fluorescence microscopy, membrane-active hIAPP species are observed through an assembly process, ranging from soluble oligomers to high-order aggregates within the membrane organization, and finally to mature amyloid fibrils. The transformation of spherical prefibrillar assemblies into elongated mature fibrils is clearly seen in the microscopy images. Membrane disruption is observed prior to the formation of straight hIAPP fibrils, reinforcing the fact that, non-fibrillar, but rather oligomeric hIAPP species are responsible for membrane destabilization. The high resolution structures of IAPP fibrils (and oligomers) are not known, although several models have been proposed [51–54]. Our data indicate that hIAPP in its oligomeric form interacts with the lipid bilayer of the liposomes, comparatively creating more ordering on the first 8 carbon positions of the acyl chain (Fig. 2C). A putative explanation would be that only a part of the hIAPP sequence may transiently interact with the beginning of the acyl chain. Interestingly, recent molecular dynamics simulations [55] showed that N-terminal residues of hIAPP facing toward the bilayer are critical for membrane insertion. In the same theoretical study, and in an earlier experimental works [43,44], the lipid composition and the presence of anionic lipids has been proven to be a relevant factor for promoting hIAPP insertion. As recently reported in two studies [32,57], the use of lipid-based systems has promising effects on the inhibition of hIAPP oligomerization and toxicity. Our approach, based on the reconstitution of liposomes of tuneable lipid composition, could ideally be used to probe different biologically-relevant lipid compositions as well as hIAPP mutants to further understand the molecular mechanism of hIAPP-membrane

insertion and potentially design lipid-based anti-amyloidogenic compounds.

Acknowledgments

This work was supported by the Science and Engineering Research Board, Govt. of India under the Young Scientist Project Grant (Grant No. SB/FT/CS-013/2013 M.S.S), Campus France (Aquitaine - Karnataka Pre-Doctoral Exchange Program to M.B.D.), the European Research Council (ERC-2015-StG GA no. 639020 to A.L.), IdEx Bordeaux (Chaire d'Installation to B.H.), ANR (ANR-14-CE09-0020-01 to A.L.) and CNRS (IR-RMN FR3050).

Appendix A. Supplementary data

Supplementary data to this article can be found online at https://doi.org/10.1016/j.bpc.2018.12.002.

References

[1] M. Sunde, et al., Common core structure of amyloid fibrils by synchrotron X-ray diffraction, J. Mol. Biol. 273 (3) (1997) 729–739.
[2] D. Eisenberg, M. Jucker, The amyloid state of proteins in human diseases, Cell 148 (6) (2012) 1188–1203.
[3] T.P. Knowles, M. Vendruscolo, C.M. Dobson, The amyloid state and its association with protein misfolding diseases, Nat. Rev. Mol. Cell Biol. 15 (6) (2014) 384–396.
[4] M.P. Lambert, et al., Diffusible, nonfibrillar ligands derived from Abeta1-42 are potent central nervous system neurotoxins, Proc. Natl. Acad. Sci. U. S. A. 95 (11) (1998) 6448–6453.
[5] D.M. Hartley, et al., Protofibrillar intermediates of amyloid beta-protein induce acute electrophysiological changes and progressive neurotoxicity in cortical neurons, J. Neurosci. 19 (20) (1999) 8876–8884.
[6] N. Cremades, S.W. Chen, C.M. Dobson, Structural Characteristics of alpha-Synuclein Oligomers, Int. Rev. Cell Mol. Biol. 329 (2017) 79–143.
[7] N. Sahara, S. Maeda, A. Takashima, Tau oligomerization: a role for tau aggregation intermediates linked to neurodegeneration, Curr. Alzheimer Res. 5 (6) (2008) 591–598.
[8] L.M. Smith, S.M. Strittmatter, Binding Sites for amyloid-beta oligomers and synaptic toxicity, Cold Spring Harb. Perspect. Med. 7 (5) (2017).
[9] K. Matsuzaki, Formation of toxic amyloid fibrils by amyloid beta-protein on ganglioside clusters, Int. J. Alzheimers Dis. 2011 (2011) 956104.
[10] L. Haataja, et al., Islet amyloid in type 2 diabetes, and the toxic oligomer hypothesis, Endocr. Rev. 29 (3) (2008) 303–316.
[11] L. Khemtemourian, E. Gazit, A. Miranker, Recent insight in islet amyloid polypeptide morphology, structure, membrane interaction, and toxicity in type 2 diabetes, J. Diabetes Res. 2016 (2016) 2535878.
[12] M. Birol, et al., Conformational switching within dynamic oligomers underpins toxic gain-of-function by diabetes-associated amyloid, Nat. Commun. 9 (1) (2018) 1312.
[13] R. Kayed, et al., Common structure of soluble amyloid oligomers implies common mechanism of pathogenesis, Science 300 (5618) (2003) 486–489.
[14] J.D. Sipe, et al., Amyloid fibril proteins and amyloidosis: chemical identification and clinical classification international society of amyloidosis 2016 nomenclature guidelines, Amyloid 23 (4) (2016) 209–213.
[15] P. Westermark, et al., A novel peptide in the calcitonin gene related peptide family as an amyloid fibril protein in the endocrine pancreas, Biochem. Biophys. Res. Commun. 140 (3) (1986) 827–831.
[16] G.J. Cooper, et al., Purification and characterization of a peptide from amyloid-rich pancreases of type 2 diabetic patients, Proc. Natl. Acad. Sci. U. S. A. 84 (23) (1987) 8628–8632.
[17] A. Clark, et al., Islet amyloid in type 2 (non-insulin-dependent) diabetes, APMIS 104 (1) (1996) 12–18.
[18] A. Clark, et al., Islet amyloid polypeptide: actions and role in the pathogenesis of diabetes, Biochem. Soc. Trans. 24 (2) (1996) 594–599.
[19] S.E. Kahn, S. Andrikopoulos, C.B. Verchere, Islet amyloid: a long-recognized but underappreciated pathological feature of type 2 diabetes, Diabetes 48 (2) (1999) 241–253.
[20] S.E. Kahn, The relative contributions of insulin resistance and beta-cell dysfunction to the pathophysiology of Type 2 diabetes, Diabetologia 46 (1) (2003) 3–19.
[21] A.E. Butler, et al., Beta-cell deficit and increased beta-cell apoptosis in humans with type 2 diabetes, Diabetes 52 (1) (2003) 102–110.
[22] P. Westermark, Quantitative studies on amyloid in the islets of Langerhans, Ups. J. Med. Sci. 77 (2) (1972) 91–94.
[23] A. Clark, et al., Islet amyloid, increased A-cells, reduced B-cells and exocrine fibrosis: quantitative changes in the pancreas in type 2 diabetes, Diabetes Res. 9 (4) (1988) 151–159.
[24] A.S. Detoma, et al., Misfolded proteins in Alzheimer's disease and type II diabetes, Chem. Soc. Rev. 41 (2) (2012) 608–621.
[25] P. Cao, et al., Islet amyloid: from fundamental biophysics to mechanisms of cytotoxicity, FEBS Lett. 587 (8) (2013) 1106–1118.
[26] A. Mukherjee, C. Soto, Prion-like protein aggregates and type 2 diabetes, Cold Spring Harb. Perspect. Med. 7 (5) (2017).
[27] A. Lorenzo, et al., Pancreatic islet cell toxicity of amylin associated with type-2 diabetes mellitus, Nature 368 (6473) (1994) 756–760.
[28] T.A. Mirzabekov, M.C. Lin, B.L. Kagan, Pore formation by the cytotoxic islet amyloid peptide amylin, J. Biol. Chem. 271 (4) (1996) 1988–1992.
[29] J. Janson, et al., The mechanism of islet amyloid polypeptide toxicity is membrane disruption by intermediate-sized toxic amyloid particles, Diabetes 48 (3) (1999) 491–498.
[30] N.B. Last, E. Rhoades, A.D. Miranker, Islet amyloid polypeptide demonstrates a persistent capacity to disrupt membrane integrity, Proc. Natl. Acad. Sci. U. S. A. 108 (23) (2011) 9460–9465.
[31] J.R. Brender, et al., Membrane disordering is not sufficient for membrane permeabilization by islet amyloid polypeptide: studies of IAPP(20-29) fragments, Phys. Chem. Chem. Phys. 15 (23) (2013) 8908–8915.
[32] M.F.M. Sciacca, et al., A blend of two resveratrol derivatives abolishes hIAPP amyloid growth and membrane damage, Biochim. Biophys. Acta Biomembr. 1860 (9) (Sep 2018) 1793–1802.
[33] J.R. Brender, S. Salamekh, A. Ramamoorthy, Membrane disruption and early events in the aggregation of the diabetes related peptide IAPP from a molecular perspective, Acc. Chem. Res. 45 (3) (2012) 454–462.
[34] A. Demuro, et al., Calcium dysregulation and membrane disruption as a ubiquitous neurotoxic mechanism of soluble amyloid oligomers, J. Biol. Chem. 280 (17) (2005) 17294–17300.
[35] E. Sparr, et al., Islet amyloid polypeptide-induced membrane leakage involves uptake of lipids by forming amyloid fibers, FEBS Lett. 577 (1–2) (2004) 117–120.
[36] J.R. Brender, et al., Membrane fragmentation by an amyloidogenic fragment of human Islet Amyloid Polypeptide detected by solid-state NMR spectroscopy of membrane nanotubes, Biochim. Biophys. Acta 1768 (9) (2007) 2026–2029.
[37] M.F. Sciacca, et al., Phosphatidylethanolamine enhances amyloid fiber-dependent membrane fragmentation, Biochemistry 51 (39) (2012) 7676–7684.
[38] J.D. Green, et al., Atomic force microscopy reveals defects within mica supported lipid bilayers induced by the amyloidogenic human amylin peptide, J. Mol. Biol. 342 (3) (2004) 877–887.
[39] P.E. Smith, J.R. Brender, A. Ramamoorthy, Induction of negative curvature as a mechanism of cell toxicity by amyloidogenic peptides: the case of islet amyloid polypeptide, J. Am. Chem. Soc. 131 (12) (2009) 4470–4478.
[40] L. Caillon, O. Lequin, L. Khemtemourian, Evaluation of membrane models and their composition for islet amyloid polypeptide-membrane aggregation, Biochim. Biophys. Acta 1828 (9) (2013) 2091–2098.
[41] B. O'Nuallain, et al., Amyloid beta-protein dimers rapidly form stable synaptotoxic protofibrils, J. Neurosci. 30 (43) (2010) 14411–14419.
[42] E.J. Alred, et al., Stability of Iowa mutant and wild type Abeta-peptide aggregates, J. Chem. Phys. 141 (17) (2014) 175101.
[43] S.A. Jayasinghe, R. Langen, Lipid membranes modulate the structure of islet amyloid polypeptide, Biochemistry 44 (36) (2005) 12113–12119.
[44] D.H. Lopes, et al., Mechanism of islet amyloid polypeptide fibrillation at lipid interfaces studied by infrared reflection absorption spectroscopy, Biophys. J. 93 (9) (2007) 3132–3141.
[45] J.A. Williamson, J.P. Loria, A.D. Miranker, Helix stabilization precedes aqueous and bilayer-catalyzed fiber formation in islet amyloid polypeptide, J. Mol. Biol. 393 (2) (2009) 383–396.
[46] M. Gao, R. Winter, The effects of lipid membranes, crowding and osmolytes on the aggregation, and fibrillation propensity of human IAPP, J. Diabetes Res. 2015 (2015) 849017.
[47] M.F. Engel, et al., Islet amyloid polypeptide inserts into phospholipid monolayers as monomer, J. Mol. Biol. 356 (3) (2006) 783–789.
[48] M. Zhang, et al., Molecular understanding of Abeta-hIAPP cross-seeding assemblies on lipid membranes, ACS Chem. Neurosci. 8 (3) (2017) 524–537.
[49] A. Rawat, et al., Aggregation-induced conformation changes dictate islet amyloid polypeptide (IAPP) membrane affinity, Biochim. Biophys. Acta 1860 (9) (Sep 2018) 1734–1740.
[50] D.K. Lee, et al., Lipid composition-dependent membrane fragmentation and pore-forming mechanisms of membrane disruption by pexiganan (MSI-78), Biochemistry 52 (19) (2013) 3254–3263.
[51] S. Luca, et al., Peptide conformation and supramolecular organization in amylin fibrils: constraints from solid-state NMR, Biochemistry 46 (47) (2007) 13505–13522.
[52] J.J. Wiltzius, et al., Atomic structures of IAPP (amylin) fusions suggest a mechanism for fibrillation and the role of insulin in the process, Protein Sci. 18 (7) (2009) 1521–1530.
[53] D.C. Rodriguez Camargo, et al., Stabilization and structural analysis of a membrane-associated hIAPP aggregation intermediate, elife 6 (2017).
[54] D.C. Rodriguez Camargo, et al., The redox environment triggers conformational changes and aggregation of hIAPP in type II diabetes, Sci. Rep. 7 (2017) 44041.
[55] M. Zhang, et al., Membrane interactions of hIAPP monomer and oligomer with lipid membranes by molecular dynamics simulations, ACS Chem. Neurosci. 8 (8) (2017) 1789–1800.
[57] X. Fang, et al., Dual effect of PEG-PE micelle over the oligomerization and fibrillation of human islet amyloid polypeptide, Sci. Rep. 8 (1) (2018) 4463.